3rd URSI AT-AP-RASC, Gran Canaria, 29 May – 3 June 2022

Characteristic Mode Analysis of SIR Coupled Dual Band Dipole Antenna

Manoj Mani*, Remsha Moolat and Mohanan Pezholil
Department of Electronics, Cochin University of Science and Technology, Kochi, India

Abstract

Characteristic mode analysis of a stepped impedance resonator (SIR) coupled dual-band dipole antenna is presented in this paper. Characteristic mode theory is effectively used to understand the resonant mechanism of the antenna. The antenna prototype is realized on the double-sided FR4 substrate of dielectric constant 4.4 and loss tangent 0.025. The proposed dual-band antenna resonates at 2.45 GHz and 5.5 GHz with an impedance bandwidth of 90 MHz and 1.6 GHz, respectively.

1 Introduction

In modern antenna engineering, the characteristic mode analysis is efficiently utilized to design and optimize antennas and antenna arrays for their clear physical insight [1-5]. The greatest advantage of characteristic mode analysis over other conventional approaches is that it can provide an excellent physical interpretation of radiating structures without excitations. This source-free method is recently used to investigate the resonant mechanism and radiation behavior of many planar antennas [6, 7]. In the present wireless communication systems, the 2.4 GHz, 5.2 GHz, and 5.8 GHz ISM bands are highly demanded and widely used for various applications such as wireless local area networks, Bluetooth, and wireless printers. Owing to the higher demand of this application bands, dual-band antennas are investigated. Planar inverted F antennas [8, 9] and slot antennas [10, 11] are designed to achieve dual-band operations. Planar inverted F antennas are realized with a large ground plane, which makes the antenna complex and bulkier. Capacitive coupling in fractal antenna offers a dual-band operation [12] and a shorted parasitic element is used to achieve a dual-band operation in monopole antenna [13]. A planar dipole antenna and a folded SIR parasitic element provide dual-band frequency. The electrical size of the antenna is very small and gives good impedance bandwidth of 90 MHz and 1.6 GHz in a lower and higher band, respectively. The characteristic mode analysis is productively utilized to explain the resonant mechanism of the proposed antenna.

2 Antenna Geometry

The geometry and optimized dimensions of the proposed SIR coupled dual-band antenna is shown in Figure 1. The antenna optimizations are performed using full-wave electromagnetic simulation software CST microwave studio. The optimized antenna is fabricated on a low-cost FR4 substrate of thickness 1.6 mm. The photograph of the fabricated prototype is shown in Figure 1(c). The proposed antenna has an overall dimension of 40 x 25 x 1.6 mm^3. The design of the antenna is started with a planar dipole antenna of length 17 mm and width of 2 mm. This planar dipole antenna resonates at 5.5 GHz. As shown in Figure 1, the dipole arm is realized as a double-sided structure to reduce the return current. The lower resonance frequency at 2.45 GHz is achieved by using a folded SIR structure as a parasitic element to the planar dipole antenna. The SIR structures have the advantages of the compact shape and spurious frequency control. The two important physical parameters, such as impedance ratio (K) and length ratio (α_l), determine the resonance frequency of a SIR. The impedance ratio and length ratio of the SIR structure can be expressed as [14].

$$K=\frac{Z_2}{Z_1} \quad (1)$$

$$\alpha_l=\frac{L_b}{L_b+L_c} \quad (2)$$

Where the Z_1 and Z_2 are the characteristic impedances of the width W_t and W_v as given in Figure 1. For the proposed design, K and α_l are 0.81 and 0.62, respectively, which resonates at 2.45 GHz.

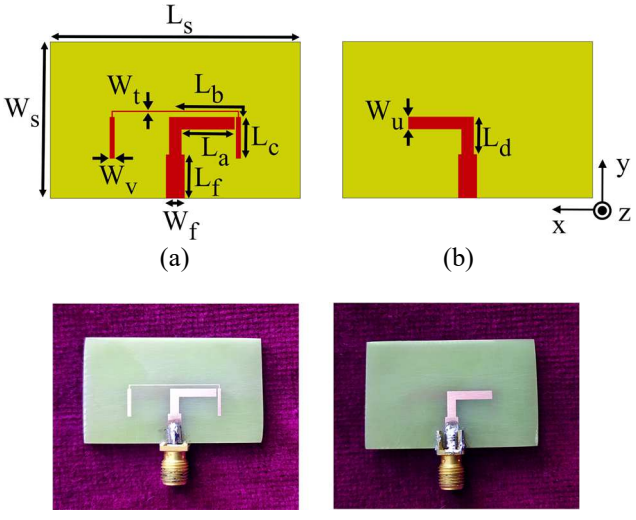

Figure 1. Geometry of the proposed antenna (a) Top view (b) Bottom view (c) Photograph of the fabricated prototype. (The optimized design parameters are L_s=40 mm, W_s=25 mm, L_a= 8.5 mm, L_b= 11.2 mm, L_c= 6.65 mm, L_d= 6 mm, L_f= 7 mm, W_f= 3 mm, W_t= 0.2 mm, W_u= 2 mm and W_v= 0.8 mm,)

3 Characteristic Mode Analysis

Characteristic mode analysis (CMA) is widely utilized to understand the radiating structures' physical mechanism [15]. CMA is a powerful tool for the design and analysis of many challenging antennas and antenna arrays. The most significant advantage of this analysis is that it can provide various inherent resonant modes and the antennas' radiation mechanism without any excitation. With this physical understanding of the antenna resonance, it is possible to optimize the antenna dimensions for desired resonant modes. This versatile modal analysis tool can also provide information regarding the feed point. Usually, the places having maximum current densities are chosen for the exact location for feed. In this study, the resonant mechanism of the dual-band antenna is analyzed using characteristic mode analysis. Three merit parameters are analyzed to explain the physical mechanism of the antenna. These parameters are eigenvalue, modal significance, and characteristic angle.

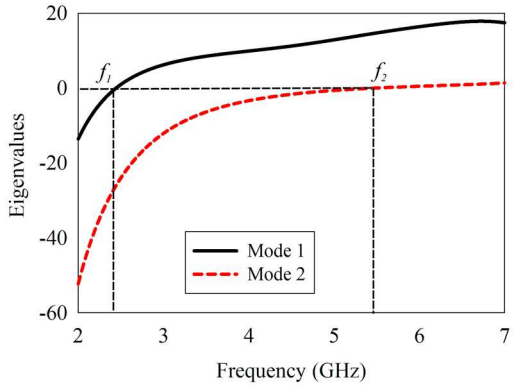

(a)

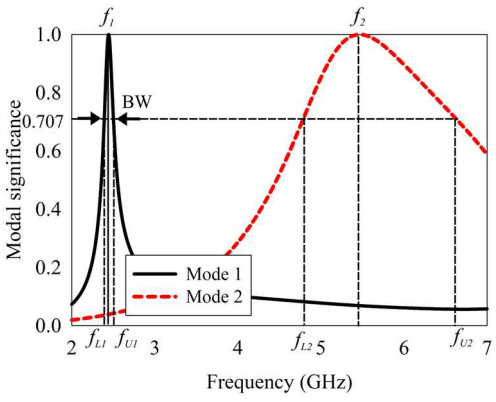

(b)

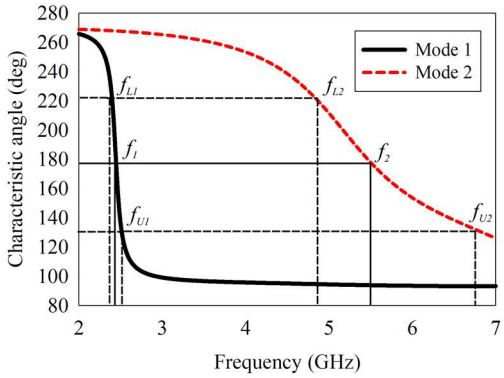

(c)

Figure 2. Characteristic mode analysis curves for the first two resonant modes of the proposed antenna. (a) Eigenvalue (b) Modal significance (c) Characteristic angles

In the characteristic mode analysis, the eigenvalues (λ_n) of the radiating structure are clearly investigated. The magnitude of the eigenvalues provides the resonance behavior of the antenna. The eigenvalue of a radiating structure ranges from -∞ to ∞. The eigenvalue represents the ratio of reactive to radiated power. When the reactive power is zero, the modes radiate efficiently. Figure 2(a) shows the variations of eigenvalues for the first two resonant modes of the proposed antenna. The resonant frequencies are obtained at 2.45 GHz and 5.5 GHz and are marked respectively as f_1 and f_2 in Figure 2(a). The mode with eigenvalues greater than zero stores the magnetic energy, and these modes are known as the inductive modes. The mode stores the electric energy when the eigenvalue less than zero, and those modes indicate the capacitive mode.

The modal significance (MS_n) provides the intrinsic property of each resonant modes, and it can be presented as [15]

$$MS_n = \left|\frac{1}{1+j\lambda_n}\right| \quad (3)$$

The modal significance equation presented in (3) transforms the huge range of eigenvalues (-∞, ∞) to a much smaller range of (0, 1). The modal significance curve for the resonant modes of the proposed antenna is shown in Figure 2(b). The mode with modal significance value one radiates efficiently. The radiating bandwidth can be calculated from half-power points (0.707). The first resonance gives a narrow impedance bandwidth of 3.6 % from 2.4 GHz (f_{L1}) to 2.49 GHz (f_{U1}), and the second resonance provides a wide bandwidth of 29.09% from 4.95 GHz (f_{L2}) to 6.55 GHz (f_{U1}). From this radiating bandwidth, the modal quality factor can be calculated and is given by

$$MQ_{factor} = \frac{1}{BW} \quad (4)$$

The modal quality factor indicates how sharp the resonance is. For the proposed design, the modal quality factor for lower resonance and higher resonance is 27.77 and 3.43, respectively.

Characteristic angle (β_n) is another crucial parameter analyzed to explain the resonant behavior of the antenna. The characteristic angle is given by

$$\beta_n = 180^0 - \tan^{-1}(\lambda_n) \quad (5)$$

The characteristic angle curve for the first two modes of the proposed antenna is shown in Figure 2(c). The frequencies correspond to the characteristic angle 180^0 gives the resonance and is marked as f_1 and f_2 at 2.45 GHz and 5.5 GHz, respectively, in Figure 2(c). The lower band (f_{L1}, f_{L2}) and upper band (f_{U1}, f_{U2}) frequencies are calculated from the characteristic angle 225^0 and 135^0 respectively [15].

The characteristic current distributions for first and second resonant frequencies are shown in Figure 3. At the lower resonance, the high impedance portion of the folded SIR parasitic element holds the maximum current and is marked as point B in Figure 3(a). In this case, the current direction along the SIR is from A to C with the maximum current at B and current nulls at points A and C. This distribution of the characteristic current contributes to the radiation at the lower resonance.

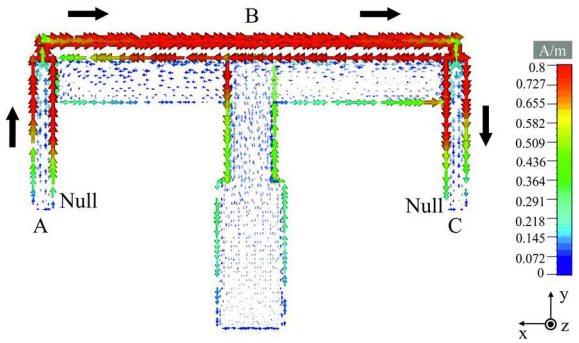

(a)

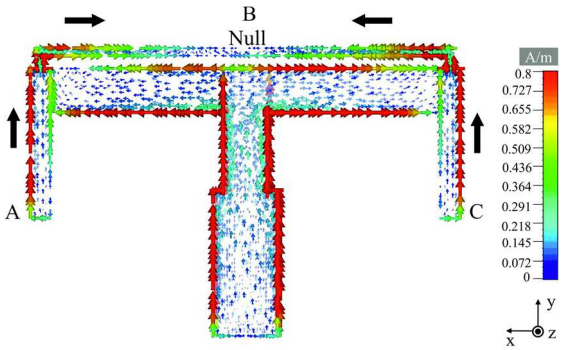

(b)

Figure 3. The characteristic current distributions of the first two resonant modes of the antenna (a) 2.45 GHz (b) 5.5 GHz.

The characteristic current distribution at the higher resonance frequency is shown in Figure 3(b). In this case, the direction of current along the SIR is from A to B and C to B. These currents cancel each other and create a null at the center. This shows that SIR parasitic element has not much impact on the higher resonance frequency. The edges of the planar dipole antenna carry the maximum current, contributing to higher resonance radiation.

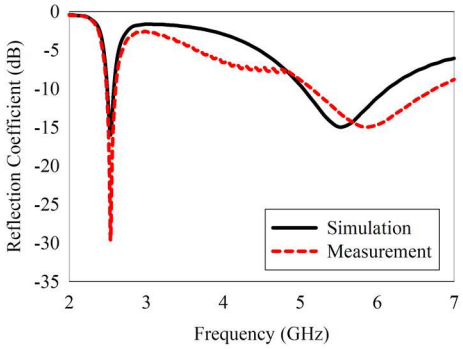

Figure 4. Simulated and measured reflection coefficient of the proposed antenna.

Figure 4 shows the simulated and measured reflection coefficients of the proposed antenna. A desirable impedance bandwidth of 90 MHz (2.4-2.49 GHz) and 1.6 GHz (4.95-6.55 GHz) is achieved at the lower and higher resonance frequencies.

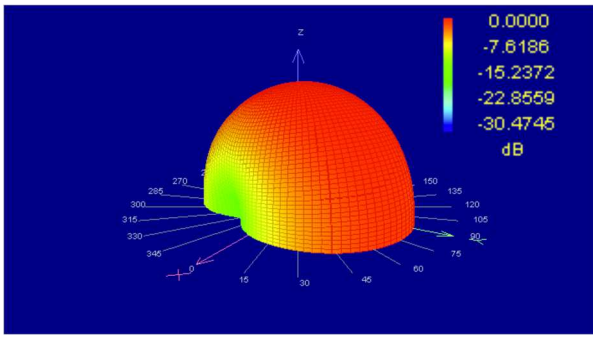

(a)

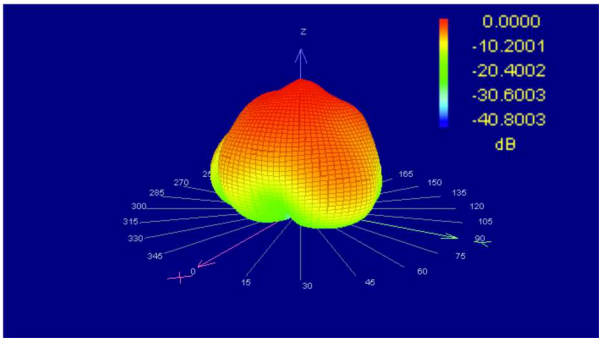

(b)

Figure 5. Measured 3D radiation pattern of the dual-band antenna using RFxpert (a) 2.45 GHz (b) 5.5 GHz.

Figure 5 shows the measured 3D normalized radiation pattern of the antenna at 2.45 GHz and 5.5 GHz. The measured radiation pattern shows that the antenna radiates omnidirectionally in the lower band and broadside at the higher band. The 3D pattern measurements are carried out using EMSCAN RFxpert.

4 Conclusion

The characteristic mode analysis of the SIR coupled dual-band dipole antenna is presented. The characteristic mode theory is productively utilized to understand the resonant mechanism of the antenna and calculated the radiating bandwidth and modal quality factor. The measured impedance bandwidth of the antenna is 90 MHz (2.4-2.49 GHz) for the first resonance and 1.6 GHz (4.95-6.55 GHz) for the second resonance, which covers the 2.4 GHz, 5.2 GHz, and 5.8 GHz ISM bands. The antenna shows an omnidirectional radiation pattern in the lower band and a broadside radiation pattern at the higher band.

5 Acknowledgements

The authors acknowledge University Grants Commission, Government of India and Department of Science and Technology (DST) for financial assistance.

6 References

1. E. Safin and D. Manteuffel, "Manipulation of characteristic wave modes by impedance loading," *IEEE Trans. Antennas Propag*., **63**, 4, Apr. 2015, pp. 1756–1764, doi: 10.1109/TAP.2015.2401586.

2. E. Antonino-Daviu, C. A. Suarez-Fajardo, M. Cabedo-Fabrés, and M. Ferrando-Bataller, "Wideband antenna for mobile terminals based on the handset PCB resonance," *Microw. Opt. Technol. Lett.,* **48**, 7, Jul. 2006, pp. 1408–1411, doi: 10.1002/mop.21654.

3. M. Bouezzeddine and W. L. Schroeder, "Design of a wideband, tunable four-port MIMO antenna system with high isolation based on the theory of characteristic modes," *IEEE Trans. Antennas Propag.,* **64**, 7, Jul. 2016, pp. 2679–2688, doi: 10.1109/TAP.2016.2543757.

4. A. A. Salih, Z. N. Chen and K. Mouthaan, "Characteristic Mode Analysis and Metasurface-based suppression of higher order modes of a 2×2 closely spaced phased array," *IEEE Trans. Antennas Propag,* **65**, 3, March 2017, pp. 1141–50, doi: 10.1109/TAP.2016.2647683.

5. T. Lonsky, P. Hazdra and J. Kracek, "Characteristic Modes of Dipole Arrays," *IEEE Antennas Wireless Propag. Lett.,* **17**, 6, June 2018, pp. 998-1001, doi: 10.1109/LAWP.2018.2828986.

6. B. R. Perli and A. M. Rao, " Characteristic mode analysis of wideband microstrip antenna," *Prog Electromagn Res C.* **97**, 11, December 2019, pp. 201–213, doi: 10.2528/PIERC19091401.

7. M. Mohamed , Elsewe and D. Chatterjee, "Characteristic mode analysis of excitation feed probes in microstrip patch antennas," *IEEE Antennas and propagation society international symposium, APSURSI Proc*. Fajardo, July 2016: pp. 33–34, doi: 10.1109/APS.2016.7695725.

8. C. F. Tseng, C. L. Huang and C. H. Hsu, "Microstrip fed monopole antenna with a shorted parasitic element for wideband application," *Prog Electromagn Res. Lett,* **7**, March 2009, pp. 115-125, doi:10.2528/PIERL09021206.

9. W. Huang, T. S. P. See and Z. N. Chen, "2.4/5-GHz dual-band PIFA for portable devices,"*APSURSI*, Washington, USA, July 2011. pp. 430-433, doi: 10.1109/APS.2011.5996736.

10. C.M. Wu, "Dual-band CPW-fed cross-slot monopole antenna for WLAN operation," *IET Microw. Antennas Propag.,* **1**, 2, May 2007, pp. 542–546, doi: 10.1049/iet-map:20050116.

11. M. J. Chiang, J. Y. Sze, and G. F. Cheng, "A compact dual-band planar slot antenna incorporating embedded metal strips for WLAN applications," *Proc. Eur. Microw. Conf. (EuMC'09)*, Rome, Italy, October 2009, pp. 221–224, doi: 10.23919/EUMC.2009.5295978.

12. N.Wongsin, T. Suangun, C.Mahatthanajatuphat and P. Akkaraekthalin, "A multiband fractal ring antenna fed by capacitive coupling," *The 8th Electrical Engineering Electronics, Computer, Telecommunications and Information Technology (ECTI) Association of Thailand - Conference 2011*, Khon Kaen, May 2011, pp. 204-207, doi: 10.1109/ECTICON.2011.5947808.

13. C. Y. Huang and P. Y. Chiu, "Dual-band monopole antenna with shorted parasitic element," *Electron. Lett.,* **41**, 21, November 2005, pp. 1154–1155, doi: 10.1049/el:20052793.

14. M. Mani, R. Moolat, K. Vasudevan, and P.Mohanan, "Harmonic Suppressed Compact Stepped Impedance Uniplanar Dipole Antenna for WLAN Applications," *Progress In Electromagnetics Res. Lett,* **79**, October 2018, pp.45-50, doi:10.2528/PIERL18080603.

15. D. Wen, Y. Hao, H. Wang and H. Zhou, "Design of a wideband antenna with stable omnidirectional radiation pattern using the theory of characteristic modes," *IEEE Trans. Antennas Propag,* **65**, 5, May 2017, pp. 2671–2676, doi: 10.1109/TAP.2017.2679767.